Published in final edited form as:
*Int J Cancer*. 2012 March 1; 130(5): 1208–1215. doi:10.1002/ijc.26126.

# Indocyanine Green Enhanced Near Infrared Laser Treatment of Murine Mammary Carcinoma

**Gal Shafirstein, D.Sc**[1,#], **Wolfgang Bäumler, PhD**[2], **Leah J Hennings, DVM**[3], **Eric R Siegel**[4], **Ran Friedman**[1], **Mauricio A Moreno, MD**[1], **Jessica Webber**[5], **Cassie Jackson**[5], and **Robert J Griffin, PhD.**[5,#]

[1]Department of Otolaryngology, University of Arkansas for Medical Sciences, 4301 West Markham, Little Rock, AR, USA

[2]Department of Dermatology, Regensburg University, Regensburg, Germany

[3]Department of Pathology, University of Arkansas for Medical Sciences, 4301 West Markham, Little Rock, AR, USA

[4]Department of Biostatistics, University of Arkansas for Medical Sciences, 4301 West Markham, Little Rock, AR, USA

[5]Department of Radiation Oncology, University of Arkansas for Medical Sciences, 4301 West Markham, Little Rock, AR, USA

## Abstract

It is well accepted that near-infrared (NIR) lasers are appropriate to ablate benign lesions and induce irreversible thermal injury in deeply seated blood vessels. At this wavelength, the laser light penetrates deep (3–5 mm) into the skin. However, many researchers have reported noticeable pain, extending from mild to severe, during and immediately following NIR laser treatment. Intravenous administration of an exogenous chromophore (indocyanine green, ICG, dye) can effectively convert NIR laser light into heat. In this approach the presence of ICG has shown to enhance thermal injury of blood vessels in the treatment of healthy tissues. However, the effectiveness of thermal injury on the regression of cutaneous carcinomas during ICG/NIR laser therapy has not been assessed. The purpose of this study was to evaluate the potential benefit of using ICG/NIR laser therapy to regress superficial carcinoma with thermal injury. Two groups of A/J mice with subcutaneous mammary adenocarcinoma tumors (7–9 mm) were irradiated with a 808-nm NIR laser preceded by tail vein injection of ICG dye or sterile saline. Histological evaluation of the subcutaneous tissue revealed minor thermal damage and necrosis in the laser/saline group and substantial damage (up to 100% necrosis) in the laser/ICG group. The laser/ICG-treated group showed a steady reduction in tumor volume compared to the laser/saline group: 48% by Day 5 ($P$=0.045) and 69%–70% by Days 8, 9, and 10 ($P$ values 0.0005 or less).

The vascular targeted ICG–NIR laser therapy appears to have potential for treating superficial tumors.

### Keywords

Indocyanine green; near infrared (NIR) laser; adenocarcinoma; thermal imaging

[*]Corresponding author: Gal Shafirstein, D.Sc., Associate Professor, Director of Translational Research, Department of Otolaryngology, Jackson T. Stephens Spine Center and Arkansas Children's Hospital, University of Arkansas for Medical Sciences, 501 Jack Stephens Drive, Little Rock, Arkansas 72205, Tel: + 1 501 526 4917, Fax: + 1 501 686 8029, Shafirsteingal@uams.edu.
[#]Principal investigators

# INTRODUCTION

## Indocyanine Green (ICG)

Indocyanine green (ICG) is a water-soluble tricarbocyanine dye (775 g/mol) that was first approved for clinical by the US Food and Drug Administration in 1956.[1] After intravenous injection, ICG is bound to plasma proteins, mainly α-lipoproteins.[2] Thus, it is mostly confined to the intravascular space, with minimal leakage, even from abnormal or fenestrated vessels.[3] Under physiological conditions, ICG is exclusively eliminated from the blood through the liver and excreted chemically unchanged into the bile.[3–6]

The absorption spectrum of ICG dissolved in plasma exhibits a strong absorption band at about 800–810 nm (near infrared, NIR, light).[7] After light absorption, the ICG molecule can follow three different pathways to deactivate its excited state. First, the absorbed energy can be converted to fluorescent light that is centered at 830 nm. The fluorescence quantum yield in albumin solution is about 4 %. This can be used for fluorescence detection of ICG in tissue, particularly to image blood vessels.[8–10] Second, a small part of absorbed light energy is transferred to ICG triplet $T_1$ state (~ 11 %, albumin solution) that can generate reactive oxygen species such as singlet oxygen.[11, 12] Third, the absorbed energy can be converted to heat inside the ICG molecule by internal conversion; due to effective internal conversion, about 85 % of absorbed light energy is converted to heat inside the molecule.[13] Therefore, heat generation is the major process after light absorption by ICG.

Following intravenous administration of ICG, treatment can be initiated by irradiating the target tissue with NIR light. Fluorescence is the primary effect at very low laser power (<10 mW/cm$^2$) and ICG concentrations of 0.1–0.2 mg/kg body weight.[14] Phototoxicity via photodynamic therapy (PDT) was proven for low power density 10 - 5 W/cm$^2$ and exposure times of seconds or minutes.[15–17] Applying these low power densities in PDT, there is hardly any temperature increase in cells or tissue detectable due to sufficient cooling via heat conduction. Therefore, it is rather unlikely that cells suffer from thermal effects. However, at high power densities (e.g. >100 W/cm$^2$) and short pulse durations in the ms range, the temperature in the target can reach high values during ms irradiation, which is used in selective photothermolysis.[18, 19] Then, thermal injury becomes the dominant effect with intravenous ICG concentration of more than >1 mg/kg and less or equal to 4 mg/kg, the maximum allowable clinical dose.[20]

Wolfe and Csaky compared the impact of diode laser treatment (810 nm, 100- to 170-mW laser power, 400-msec pulse duration, 75-μm spot size) immediately after ICG administration (75 mg/ml) to diode laser treatment alone on rat retinal arterioles using fluorescence and electron microscopy.[21] In this model, ICG-mediated diode laser irradiation induced complete vessel closure (5/5 vessels), which lasted for at least 24 hours. In comparison, diode laser irradiation without ICG only resulted in partial retinal arteriolar closure in 3/5 pigmented animals and had no effect in unpigmented animals. Electron microscopy revealed an intraluminal clot following ICG and NIR laser irradiation.

Mordon et al. performed diode laser irradiation (805 nm, 0.8-W laser power, 1.3-mm spot size, 1–5-sec pulse duration, 60–300-J/cm$^2$ fluence) 30 min after ICG application (15 mg/kg body weight in aqueous solution versus in emulsion) in the hamster skin flap model.[22] Afterwards, they evaluated the macroscopic and histological effects (2 h after irradiation) in 38 blood vessels for both ICG formulations. Using ICG in aqueous solution, a minimum energy density of 240 J/cm$^2$ was required for vessel ablation, whereas, when using ICG in emulsion, 120 J/cm$^2$ was sufficient for selective vessel ablation. Vessel diameters were not specified in this study.[22] These relatively high laser energies were required due to the low power (0.8 W) used. We showed that, when using high laser power (500 W), the energy

densities of 10.6 and 30 J/cm$^2$ and pulse times of 10–30 ms or about 1000 W/cm$^2$, are sufficient to destroy blood vessels (within the range of 20–170 μm) after administration of the maximum clinically approved dose of 2–4 mg/kg ICG.[20] In-vitro increases in cell killing with ICG photodynamic therapy (PDT) with 830-nm laser has been reported in multiple cell lines including melanoma, pancreatic cancer cells and squamous cell carcinoma.[15, 23–25]

Earlier pilot studies demonstrated that NIR diode laser system in a continuous wave mode (3–5 W/cm$^2$; 100 J/cm$^2$) in conjunction with intravenous administration of 2–4 mg/kg body weight of ICG can be used to induce tumor regression on AIDS-associated cutaneous Kaposi's sarcoma.[17, 26] Although the mechanisms inducing tissue damage were not ultimately determined, the relatively low power density suggests that phototoxicity was the main reason for tumor regression. Clinical response with ICG PDT has been also documented in-vivo for patients with cutaneous metastasis of rectal carcinoma.[27]

Although the ICG is not specifically taken up by tumor, few researchers, that studied the kinetics of ICG *in vivo*, demonstrated that ICG accumulates in breast cancer and melanoma.[28, 29] Thus, we can expect to observe higher concentration of ICG at the tumor site compared to other normal tissues.

The purpose of this study was to investigate the potential use of ICG to enhance high power NIR laser to significantly regress solid tumors via thermal injury. The primary advantage of thermal injury is the short treatment time per pulse (<0.5 second) in comparison to phototoxicity (>20 seconds). In this study, i*n vivo* thermal measurements and tumor response, as well as pathological examinations, were used to assess the effectiveness of combined ICG-NIR laser thermal therapy.

## METHODS AND MATERIALS

The study consisted with two sets of experiments. In the first set, the clearance rate of ICG in live mice was determined by monitoring the fluorescence intensity of ICG *in vivo*. In the second set of experiments, we determined the efficacy of ICG solution in enhancing near-infrared (NIR) laser thermal ablation of SCK tumors in a mouse model.

### Clearance rate of Indocyanine green (ICG), *in vivo*

ICG was obtained from Pulsion (Pulsion Medical Systems, Munich Germany) in vials of 25 mg. The ICG powder was dissolved in 5 ml sterile water and further diluted in sterile saline to a concentration of 1.25 mg/mL. A single dose of ICG solution (4 mg/kg body weight) was administered to each mouse, for imaging only. Kodak *in-vivo* imaging system (Carestream Health Molecular Imaging, New Haven, CT) was used to excite and monitor the ICG fluorescence intensity within the anesthetized mouse. The fluorescence intensity was recorded by taking consecutive images of the mice immediately before and up to 15 minutes post ICG administration. The change of the fluorescence intensity (FI) was determined by calculating the ratio between the FI at each time point t=ti>0 ($I_p$) and the FI prior to the ICG administration ($I_b$), i.e. $I_p(t=ti)/I_b(t=0)$. The image analysis and calculation were conducted with the Matlab image processing toolbox (Matlab™, Mathworks Inc. Natick, MA). The calculated change in FI was plotted as function of time. In this analysis, we assumed that the change in the FI is directly proportional to the change of the ICG concentration.

### NIR laser treatment preceded by ICG administration

In this set of experiments, the study objective was to determine the efficacy of ICG administration in enhancing tumor ablation during NIR laser irradiation of solid tumors in a mouse model.

### Animal preparation and treatment

SCK mammary carcinoma tumor cells were subcutaneously inoculated in A/J mice. Briefly, SCK cells in exponential growth phase were trypsinized and washed with serum-free medium. The mice were then injected subcutaneously with $2 \times 10^5$ cells in 0.05 mL of serum-free medium into the right rear limb. Within 1–2 weeks, the tumors size reached 7–9 mm in diameter, at which time the mice were randomized and divided into a control group (n=3) and two study groups (n=9 for ICG/laser and n=12 for the saline/laser). In the two study groups, the mice were treated with NIR laser preceded by an intravenous administration of sterile ICG solution (group 1) or sterile buffered saline (group 2), as described below. No treatment was applied to the mice in the control group.

One minute prior to laser irradiation, a single dose of 4 mg/kg (i.e. 3.2 mL/kg) of ICG solution was administered into the lateral tail vein of each mouse in the first study group. In the second study group, a single dose (of 3.2 mL/kg) of sterile saline was injected into the tail vein of each mouse. During laser treatments, the mice were anesthetized with isoflurane by inhalation. The body temperature of the mice was maintained by individually placing them on a 37 °C heated platform during treatment. Following laser treatment, the mice were allowed to recover and returned to the colony. The mice were monitored for behavior and tumor volumes for up to 10 days post treatment. Tumor sizes were measured every 1 to 3 days with a Vernier caliper. Tumor volumes were calculated using the formula $a^2b/2$, where $a$ and $b$ are the shorter and longer diameters of the tumor, respectively.

Cohorts of 3 mice from each study group were sacrificed, at day 1 and 7, post laser treatments for histological analysis. Immediately following euthanasia, the tumors were excised and were processed and embedded in paraffin blocks for routine histological analysis. Tissue slides (5 μm thick) were stained with hematoxylin and eosin (H&E) and examined under a light microscope by a veterinary pathologist. Quantitative pathological analysis hardware and software, Aperio Scanscope T2 and ImageScope software (Aperio, Vista, CA), was used to determine the relative necrotic area in each tissue section.

### Laser treatment

A NIR laser system (JOLD-140-CPXF-2P A, Jenoptik Laserdiode GmbH, Jena, Germany) emitting at a wavelength of 808 nm was used in this study. The laser beam diameter was 5 mm, the pulse time was 0.2 seconds, and the laser power output was 85 W. The laser hand-piece was positioned above and perpendicular to the heated platform on which the mouse was placed. The platform was attached to a micrometer-driven translation stage. The entire tumor and margins were irradiated by moving the stage at 2.5 mm increments (in the x and y direction) while the laser beam was stationary. At each increment, one laser pulse was delivered to the tumor, resulting in complete coverage of the tumor region with 50% overlap between pulses. Epidermal cooling was accomplished by applying ultrasonic transmission gel (Parker Laboratories, Fairfield, NJ) at 2 °C to the skin, for 1 minute prior to the laser treatment.

The temperature changes during the laser treatment were monitored with an infrared camera (Thermovision A20, FLIR, Boston, MA). The IR images were recorded at a rate of 70 frames per second during the laser irradiation and as long as 3 seconds after the laser pulse was delivered. Although the thermal camera detects temperature from <0.3 mm below the skin surface, we stipulate that the relative change in the surface temperature is directly proportional to the temperature changes within the tumor during laser therapy. The thermal measurements were used to compare the different temperature profile in response to laser therapy.

### Statistical analysis

Tumor volumes were calculated from long and short diameters measured every 1–3 days, summarized by Day and Treatment as means and standard deviations (SDs), and analyzed for treatment differences over time via mixed-models repeated-measures analysis. The repeated-measures autocovariance followed a first-order autoregressive structure with unequal variances both over time and between treatment groups, and the Satterthwaite method was accordingly used to determine error degrees of freedom in all estimates and comparisons. The significance level was set at $P<0.05$ despite the multiple comparisons, so as not to inflate Type II error in this low-powered feasibility study.

## RESULTS

### Clearance rate of ICG, *in vivo*

Figure 1 presents the average change of FI within a region of interest (ROI) around the tumor. A rapid increase of the FI was observed within the first 1.5 minutes, followed by slower accumulation rate up to 6 minutes, post injection, and constant FI up to 15 minutes post injection. Each data point is an average of FI measurements taken from 3 different animals. The error bars (in figure 1) are of one standard deviation from the mean value of the FI.

### NIR laser irradiation preceded by ICG administration

The temperature map at the end of the laser pulse for mice that were injected with ICG is shown in Figure 2. The average temperature increase, at the surface, as a function of time is shown in Figure 3. In this figure each point is the mean temperature from measurements taken at the same time point in different regions and different animals (i.e. we averaged the results after we collected the measurements). The relaxation time in both groups was 3 seconds. However, a rapid heating was observed in mice from the ICG-treated group, and the average maximum surface temperature was about 12 °C higher in this group compared to the saline-treated group.

Tumors growing in mice that were not laser-irradiated increased their volume 4× in only 7 days (Griffin, 1999, 2000).[30, 31] In laser-irradiated mice, means and SDs of tumor volume are shown in Figure 4. Mean volumes in the laser/saline group increased steadily, from 160 $cm^3$ on Day 1 to more than 800 $cm^3$ by Day 10, whereas mean volumes in the laser/ICG group increased to a maximum of 260 $cm^3$ at Day 5 followed by a slight decline, such that differences between the groups increased steadily over time. Percent decreases (*P* values) in the laser/ICG group compared to laser/saline were 34% ($P=0.12$) on Day 2, 48% ($P=0.045$) on Day 5, 69% ($P=0.0005$) on Day 8, 70% ($P<0.0001$) on Day 9, and 69% ($P<0.0001$) on Day 10.

### Pathological results

The histological results from tumors taken at 24 hours after laser exposure for ICG/laser, saline/laser and an untreated control tumor is shown in figure 5. Nearly complete necrosis was observed in sections from tissues that were collected from the mice treated with ICG/laser (Figure 5) Loss of tissue architecture is present in the entire tumor at low magnification. (Figure 5A). High magnification of necrotic tumor demonstrates cellular features of necrosis, including loss of cytoplasmic and nuclear detail (Figure 5B). Significant damage to the vascular wall in peritumoral vessels, including endothelial cell necrosis and loss of endothelial cells (Figure 5C, thin arrow) and fibrin deposition (Figure 5C, thick arrow) was also observed. Fibrin deposition indicates that the endothelium is disrupted and clotting factors have been released by damaged endothelial cells. This is the first step in vascular thrombosis. Tumors treated with saline/laser demonstrated some

evidence of ablation, but substantially less than observed in the ICG treated tumors (Figure 5D). Architecture is preserved in viable regions (Figure 5D, arrow). Compared to necrotic tumor cells (Figure 5E, left), viable cells (Figure 5E, right) demonstrate maintenance of tissue architecture and nuclear and cytoplasmic detail. Vessel walls are intact, but inflammatory cells (neutrophils) are present (Figure 5F, arrows). As a reference, minimal necrosis was observed in an untreated control tumor (Figure 5 G, H), and blood vessels appeared typical of fast growing experimental tumors such as the SCK model (Figure 5 I).

## Discussion

The objective of this study was to investigate the ability of a laser treatment combined with ICG administration to ablate tumors grown from the SCK murine mammary carcincoma. As shown in previous published studies, the ICG chromophore enhances the vascular injury when irradiated with near infrared laser light.[20–22] The absorption coefficient of plasma and blood components to 808-nm wavelength is about 7% of the ICG dye at 4 mg/kg body weight of mice.[20] Furthermore, the ICG converts 85% of the NIR (808 nm) laser energy into heat. Therefore, we expected to observe higher temperatures during laser irradiation of blood vessels containing ICG in comparison to those which do not contain ICG if we were able to deliver the ICG to the tumor vasculature and/or the tumor perivascular space.

The fluorescence images in figure 1 confirmed that the ICG concentration at the tumor site was maintained for up to 15 minutes, sufficient time to treat large tumor in the clinical settings. The treatment of an individual mouse was completed within <2 minutes. Within this time frame, the concentration level of the administered ICG was at maximum level. Therefore, we can safely assume that the concentration of ICG did not change during laser treatment. Although there is no preferential uptake of the ICG by the tumor or cancer cells, the typical leaky and damaged blood vessels in the tumor could cause higher extravascular accumulation of ICG, which would explain the relatively constant FI up to 15 minutes post injection. This result is in agreement with Thayer, Unlu et al. 2010 who showed that ICG may accumulate 1.5 to 3 times more in tumor versus healthy tissue.[29]

Our group has previously shown that the laser pulse duration is a more significant factor than ICG concentration to achieve complete destruction of blood vessels.[20] However, longer pulse time could lead to skin damage as reported by Mordon et. al.[22] In the initial stages of this study we observed some degree of skin damage (data not shown) following laser irradiation in mice that received intravenous administration of ICG. The damage was found to be avoidable by employing efficient epidermal skin cooling. In our study, this was accomplished by applying pre-cooled ultrasonic gel, at 2 °C to the skin for 1 minute prior to laser treatment. Other methods such as a cool sapphire tip and cryogen spray cooling can be used to effectively protect the epidermis during laser therapy.[17, 26] Regardless of which cooling method is used to protect the epidermis from superficial thermal damage, it is imperative to do so during ICG-mediated laser therapy.

The tumor-growth delay data shows that laser/ICG had a greater effect on the tumor growth delay in comparison to the laser/saline therapy. We attribute this effect to an increase thermal damage in the tumor site during laser/ICG therapy as evident by the higher temperature recorded in the thermal imaging, during treatment. It is also possible that some degree of laser/ICG phototoxicity enhanced tumor regression; however, considering the marked differences we measured in tumor heating when ICG was injected it appears that a major portion of the therapeutic effect was mediated by thermal damage.

The histological analysis that we performed indicated nearly complete thermal ablation of tumors after ICG/laser treatment and supports the tumor growth delay observations. The

tumors were excised and processed at 1 and seven days following treatment, and the degree of necrosis at 1 week indicates that the vascular damage observed in many regions of the tumor at 1 day was irreversible. Our findings confirm the notion that ICG enhanced NIR laser photothermolysis of solid tumors, in comparison to saline/laser. Therefore, these results can be interpreted to reflect the general mechanisms at play with ICG-induced thermal destruction of tumor vasculature.

The light penetration is a function of the absorption and the reduced scattering coefficient within blood vessels and the connective tissue. In this study the majority of the ICG was confined to the blood vessels. Assuming that about 20% of the tumor volume consists of blood vessels, the light penetration will be reduced by about 20%, at most. NIR light penetrates about 5 mm of tissue. Therefore, we would expect that a penetration depth of 3–4 mm was accomplished in this setting. The histological samples confirmed this assessment (figure 5) and it is in agreement with the 3.5 mm penetration depth that was observed in a clinical trial where ICG-NIR laser was used to treat Kaposi's sarcoma.[17]

Several studies have recently suggested that the stromal compartment (connective tissue) may play an important role in tumor growth. [32, 33] Therefore, we suggest that even complete thermal injury of the vascular bed, the target tissue in selective photothermolysis, may not be sufficient to induce entire tumor ablation or prevent recurrence. To further enhance tumor ablation, we are working to enhance laser absorption of the target tumor and connective tissue by increasing the extravascular concentration of ICG. We have extensively studied the use of loco-regional hyperthermia at 40–42 °C to improve perfusion and permeability of blood vessels in the tumor. [34–36] Our ongoing studies are investigating the potential of improving ICG delivery to tumor interstitial space by local hyperthermia exposure of the tumor.

In the present study the SCK mammary carcinoma model was utilized to assess the effect of ICG and NIR laser. This rapidly growing tumor has a high perfusion index, significant vascular abnormalities and hypoxia with marked metastatic potential. Some of the characteristics of this model such as regional hyperperfusion, abnormal angiogenesis and local hypoxia are shared by other highly vascular tumors such as Kaposi's sarcoma that are amenable for this therapy,[37] making our animal model a valid surrogate to study the effects of ICG and NIR laser on tumor response.

## CONCLUSION

Intravenous administration of 4 mg/kg ICG one minute before NIR laser exposure significantly enhanced thermal ablation of tumors. Our histological data suggest that the presence of ICG imparted irreversible damage to most blood vessels in the tumor, during NIR laser irradiation. Further study of this strategy is highly warranted for determining optimal number of treatments and methods for improved delivery of ICG for even greater efficacy.

## Acknowledgments

This study was supported in part by the Arkansas Children's Hospital Research Institute through the Children's University Medical Group research award (G. Shafirstein) and by NIH grants CA44114 and Central Arkansas Radiation Therapy Institute (R. Griffin). We thank Pulsion Medical Systems, Munich Germany, for providing the ICG clinical grade dye that was used in this study.

## References


1. Fox I, Brooker L, Heseltine D, Essex H, Wood E. New dyes for continuous recording of dilution curves in whole blood independent of variations in blood oxygen saturation. Am J Physiol. 1956; 187:599.
2. Muckle TJ. Plasma proteins binding of indocyanine green. Biochem Med. 1976; 15:17–21. [PubMed: 942422]
3. Paumgartner G. The handling of indocyanine green by the liver. Schweiz Med Wochenschr. 1975; 105:1–30. [PubMed: 1135620]
4. Lund-Johansen P. The dye dilution method for measurement of cardiac output. Eur Heart J. 1990; 11 Suppl I:6–12. [PubMed: 2092991]
5. Haller M, Akbulut C, Brechtelsbauer H, Fett W, Briegel J, Finsterer U, Peter K. Determination of plasma volume with indocyanine green in man. Life Sci. 1993; 53:1597–1604. [PubMed: 8231637]
6. Hetz H, Faybik P, Berlakovich G, Baker A, Bacher A, Burghuber C, Sandner SE, Steltzer H, Krenn CG. Molecular adsorbent recirculating system in patients with early allograft dysfunction after liver transplantation: a pilot study. Liver Transpl. 2006; 12:1357–1364. [PubMed: 16741899]
7. Landsman ML, Kwant G, Mook GA, Zijlstra WG. Light-absorbing properties, stability, and spectral stabilization of indocyanine green. J Appl Physiol. 1976; 40:575–583. [PubMed: 776922]
8. Desmettre T, Devoisselle JM, Mordon S. Fluorescence properties and metabolic features of indocyanine green (ICG) as related to angiography. Surv Ophthalmol. 2000; 45:15–27. [PubMed: 10946079]
9. Unno N, Inuzuka K, Suzuki M, Yamamoto N, Sagara D, Nishiyama M, Konno H. Preliminary experience with a novel fluorescence lymphography using indocyanine green in patients with secondary lymphedema. J Vasc Surg. 2007; 45:1016–1021. [PubMed: 17391894]
10. Zhu L, Zheng Y, von Kerczek CH, Topoleski LD, Flower RW. Feasibility of extracting velocity distribution in choriocapillaris in human eyes from ICG dye angiograms. J Biomech Eng. 2006; 128:203–209. [PubMed: 16524331]
11. Reindl S, Penzkofer A, Gong SH, Landthaler M, Szeimies RM, Abels C, Baumler W. Quantum yield of triplet formation for indocyanine green. Journal of Photochemistry and Photobiology A: Chemistry. 1997; 105:65–68.
12. Baumler W, Abels C, Karrer S, Weiss T, Messmann H, Landthaler M, Szeimies RM. Photo-oxidative killing of human colonic cancer cells using indocyanine green and infrared light. Br J Cancer. 1999; 80:360–363. [PubMed: 10408838]
13. Philip R, Penzkofer A, Bäumler W, Szeimies R, Abels C. Absorption and fluorescence spectroscopic investigation of indocyanine green. Journal of Photochemistry and Photobiology A Chemistry. 1996:137–148.
14. Akorn. Buffalo Grove, IL 60089: Drug insert for indocyanine and green Akorn, Inc; 2004.
15. Abels C, Fickweiler S, Weiderer P, Baumler W, Hofstadter F, Landthaler M, Szeimies RM. Indocyanine green (ICG) and laser irradiation induce photooxidation. Arch Dermatol Res. 2000; 292:404–411. [PubMed: 10994775]
16. Engel E, Schraml R, Maisch T, Kobuch K, Konig B, Szeimies RM, Hillenkamp J, Baumler W, Vasold R. Light-induced decomposition of indocyanine green. Invest Ophthalmol Vis Sci. 2008; 49:1777–1783. [PubMed: 18436812]
17. Abels C, Karrer S, Baumler W, Goetz AE, Landthaler M, Szeimies RM. Indocyanine green and laser light for the treatment of AIDS-associated cutaneous Kaposi's sarcoma. Br J Cancer. 1998; 77:1021–1024. [PubMed: 9528851]
18. Anderson RR. Lasers in dermatology--a critical update. J Dermatol. 2000; 27:700–705. [PubMed: 11138535]
19. Anderson RR, Parrish JA. Selective photothermolysis: precise microsurgery by selective absorption of pulsed radiation. Science. 1983; 220:524–527. [PubMed: 6836297]
20. Babilas P, Shafirstein G, Baier J, Schacht V, Szeimies RM, Landthaler M, Baumler W, Abels C. Photothermolysis of blood vessels using indocyanine green and pulsed diode laser irradiation in the dorsal skinfold chamber model. Lasers Surg Med. 2007; 39:341–352. [PubMed: 17457841]

21. Wolfe JD, Csaky KG. Indocyanine green enhanced retinal vessel laser closure in rats: histologic and immunohistochemical observations. Exp Eye Res. 2004; 79:631–638. [PubMed: 15500822]
22. Mordon S, Desmettre T, Devoisselle JM, Mitchell V. Selective laser photocoagulation of blood vessels in a hamster skin flap model using a specific ICG formulation. Lasers Surg Med. 1997; 21:365–373. [PubMed: 9328984]
23. Tseng WW, Saxton RE, Deganutti A, Liu CD. Infrared laser activation of indocyanine green inhibits growth in human pancreatic cancer. Pancreas. 2003; 27:e42–e45. [PubMed: 14508139]
24. Urbanska K, Romanowska-Dixon B, Matuszak Z, Oszajca J, Nowak-Sliwinsk P, Stochel G. Indocyanine green as a prospective sensitizer for photodynamic therapy of melanomas. Acta Biochim Pol. 2002; 49:387–391. [PubMed: 12362980]
25. Mamoon AM, Gamal-Eldeen AM, Ruppel ME, Smith RJ, Tsang T, Miller LM. In vitro efficiency and mechanistic role of indocyanine green as photodynamic therapy agent for human melanoma. Photodiagnosis Photodyn Ther. 2009; 6:105–116. [PubMed: 19683211]
26. Szeimies RM, Lorenzen T, Karrer S, Abels C, Plettenberg A. [Photochemotherapy of cutaneous AIDS-associated Kaposi sarcoma with indocyanine green and laser light]. Hautarzt. 2001; 52:322–326. [PubMed: 11382123]
27. Karrer S, Abels C, Baumler W, Steinbauer M, Landthaler M, Szeimies RM. [Photochemotherapy with indocyanine green in cutaneous metastases of rectal carcinoma]. Dtsch Med Wochenschr. 1997; 122:1111–1114. [PubMed: 9340251]
28. Stoffelns BM. [Kinetics of indocyanine green (ICG) and clinical use for enhancement of transpupillary thermotherapy (TTT) in hypopigmented small choroidal melanomas]. Klin Monbl Augenheilkd. 2004; 221:374–378. [PubMed: 15162284]
29. Thayer D, Unlu MB, Lin Y, Yan K, Nalcioglu O, Gulsen G. Dual-contrast dynamic MRI-DOT for small animal imaging. Technol Cancer Res Treat. 2010; 9:61–70. [PubMed: 20082531]
30. Griffin RJ, Lee SH, Rood KL, Stewart MJ, Lyons JC, Lew YS, Park H, Song CW. Use of arsenic trioxide as an antivascular and thermosensitizing agent in solid tumors. Neoplasia. 2000; 2:555–560. [PubMed: 11228548]
31. Griffin RJ, Okajima K, Ogawa A, Song CW. Radiosensitization of two murine tumours with mild temperature hyperthermia and carbogen breathing. Int J Radiat Biol. 1999; 75:1299–1306. [PubMed: 10549607]
32. Gupta GP, Massague J. Cancer metastasis: building a framework. Cell. 2006; 127:679–695. [PubMed: 17110329]
33. Norton L, Massague J. Is cancer a disease of self-seeding? Nat Med. 2006; 12:875–878. [PubMed: 16892025]
34. Griffin RJ, Okajima K, Barrios B, Song CW. Mild temperature hyperthermia combined with carbogen breathing increases tumor partial pressure of oxygen (pO2) and radiosensitivity. Cancer Res. 1996; 56:5590–5593. [PubMed: 8971160]
35. Song CW, Park H, Griffin RJ. Improvement of tumor oxygenation by mild hyperthermia. Radiat Res. 2001; 155:515–528. [PubMed: 11260653]
36. Griffin RJ, Ogawa A, Williams BW, Song CW. Hyperthermic enhancement of tumor radiosensitization strategies. Immunol Invest. 2005; 34:343–359. [PubMed: 16136785]
37. Leu AJ, Yanar A, Jost J, Hoffmann U, Franzeck UK, Bollinger A. Microvascular dynamics in normal skin versus skin overlying Kaposi's sarcoma. Microvasc Res. 1994; 47:140–144. [PubMed: 8022311]

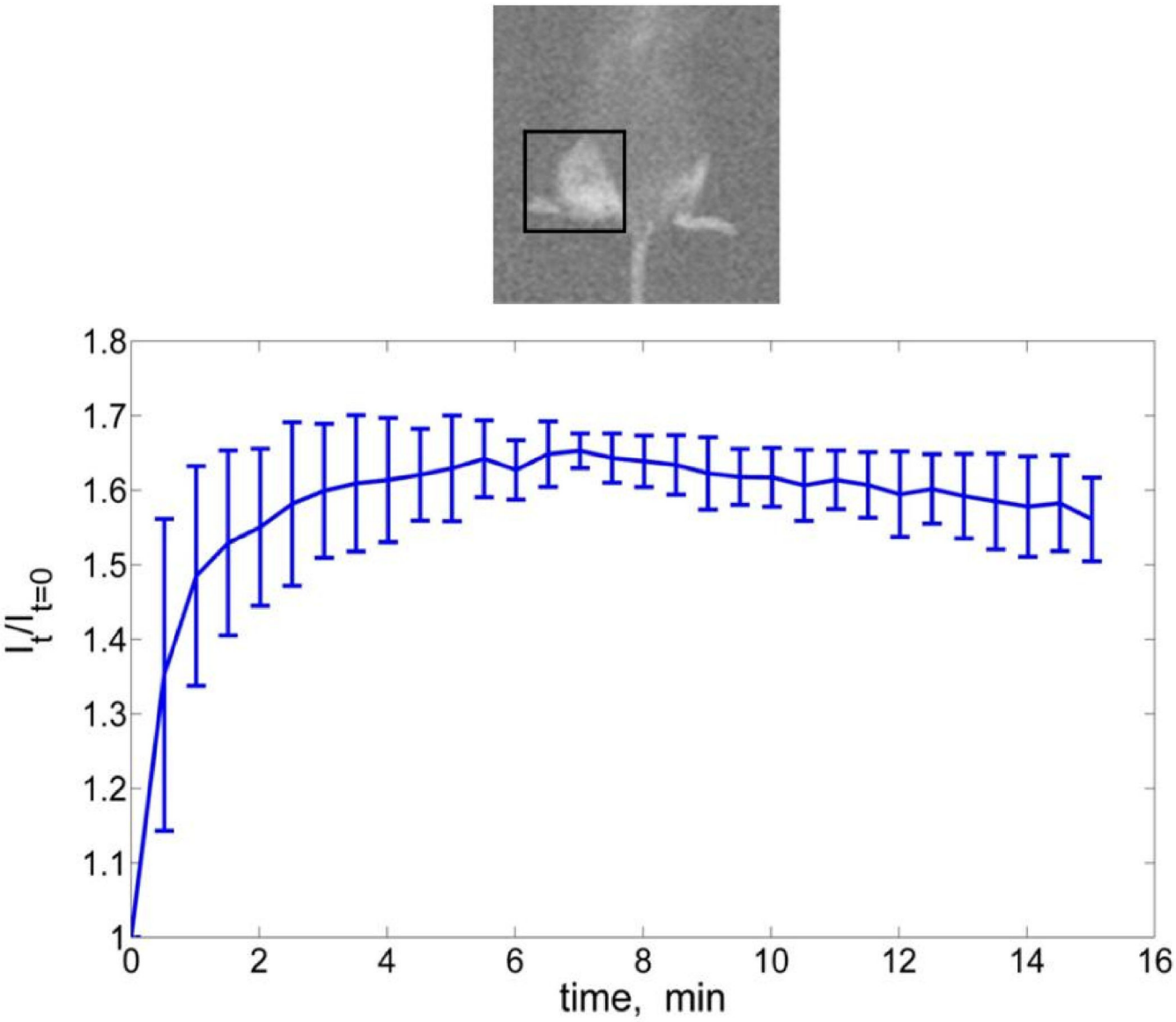


**Figure 1.**

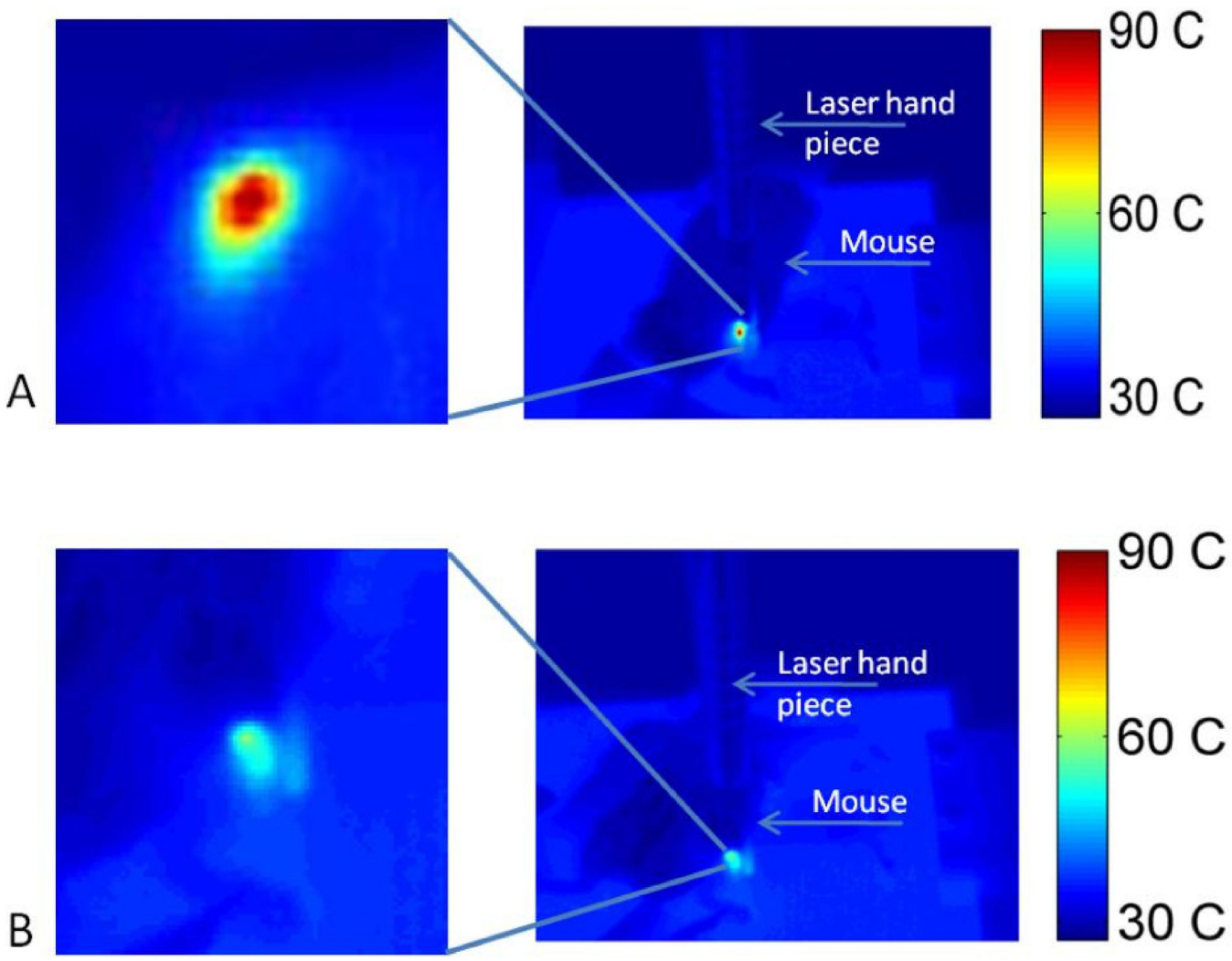


**Figure 2.**

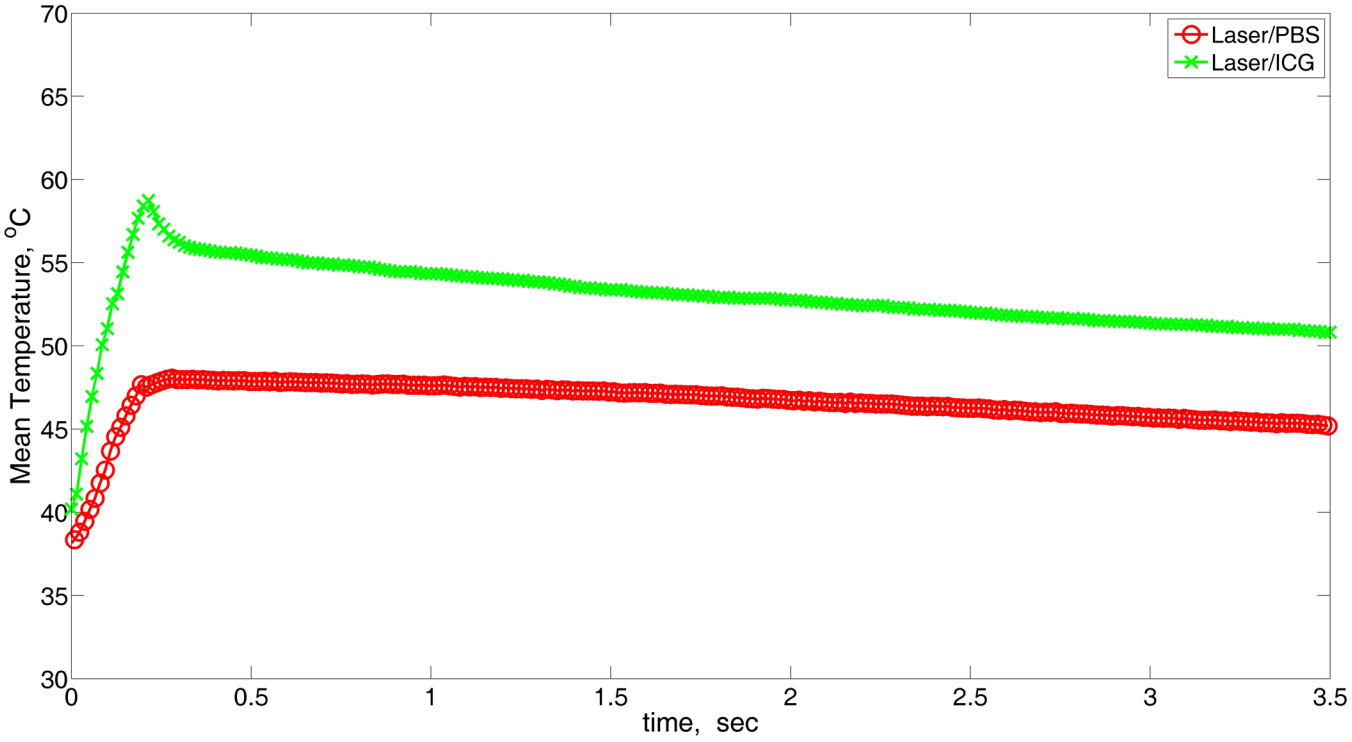


**Figure 3.**

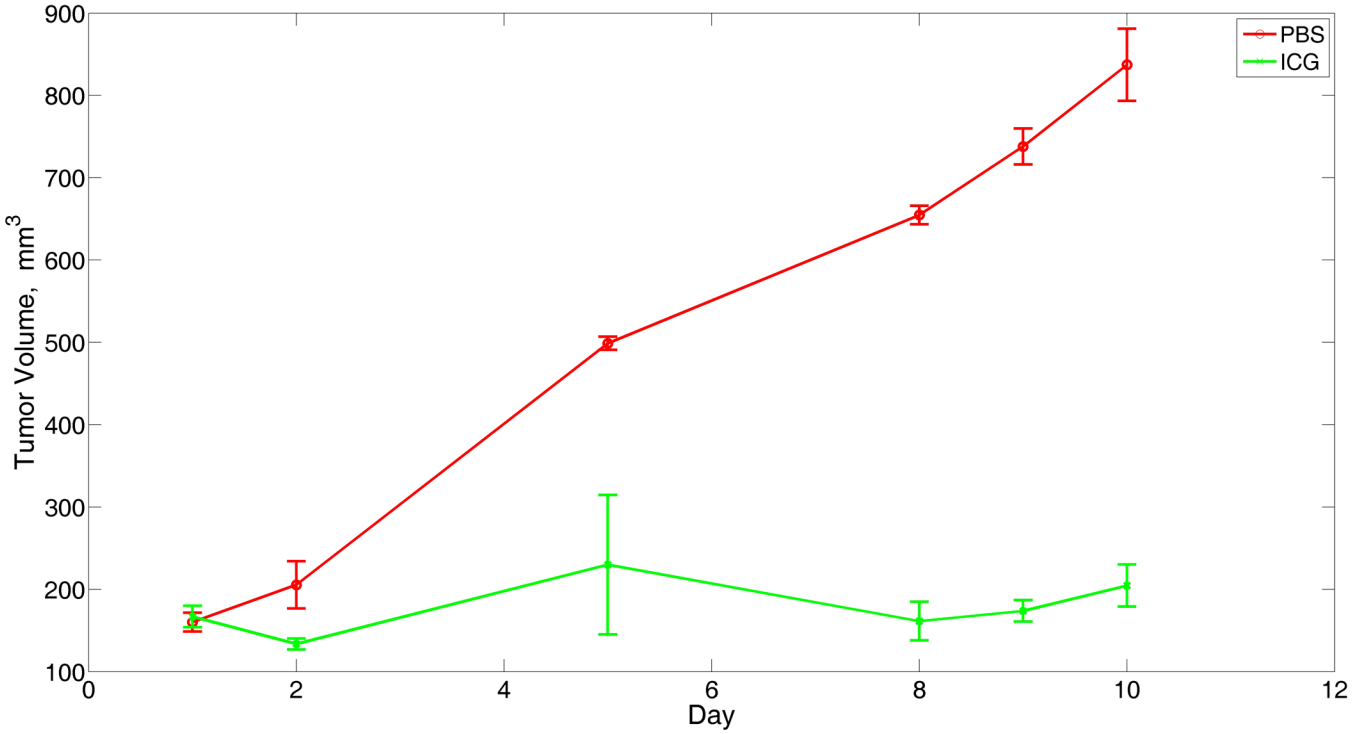


**Figure 4.**

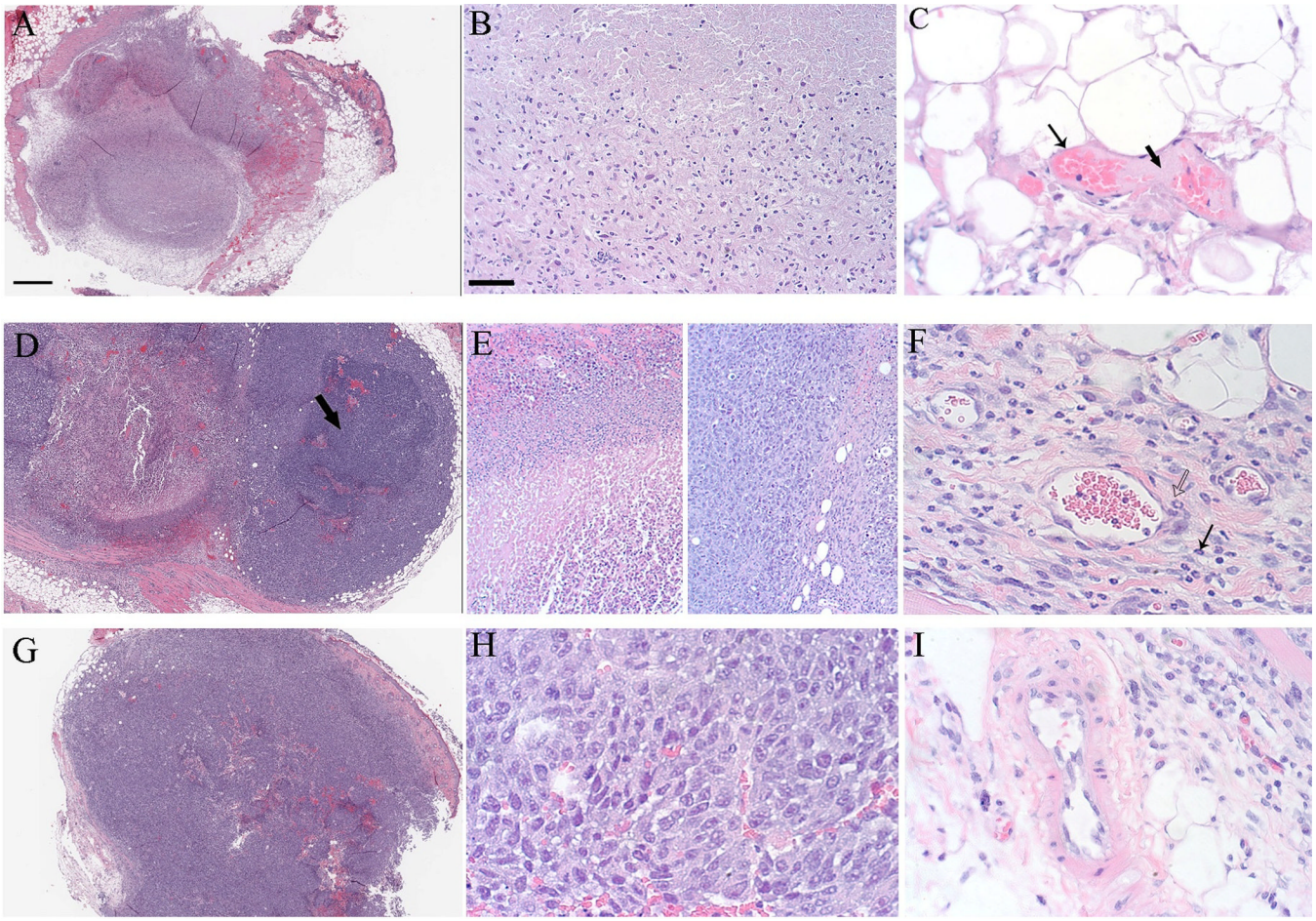


**Figure 5.**